

Preparation and Regulating Cell Adhesion of Anion-Exchangeable Layered Double Hydroxide Micropatterned Arrays

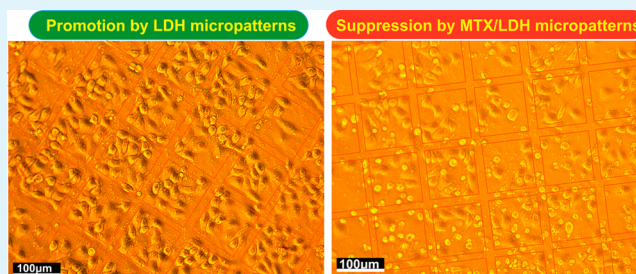
Feng Yao,^{†,‡} Hao Hu,^{†,‡} Sailong Xu,^{*,‡} Ruijie Huo,[‡] Zhiping Zhao,[‡] Fazhi Zhang,[‡] and Fujian Xu^{*,‡,§,⊥}

[‡]State Key Laboratory of Chemical Resource Engineering, [§]Key Laboratory of Carbon Fiber and Functional Polymers, Ministry of Education, College of Materials Science & Engineering, and [⊥]Beijing Laboratory of Biomedical Materials, Beijing University of Chemical Technology, Beijing 100029, China

S Supporting Information

ABSTRACT: We describe a reliable preparation of MgAl-layered double hydroxide (MgAl-LDH) micropatterned arrays on gold substrate by combining SO_3^- -terminated self-assembly monolayer and photolithography. The synthesis route is readily extended to prepare LDH arrays on the SO_3^- -terminated polymer-bonded glass substrate amenable for cell imaging. The anion-exchangeable MgAl-LDH micropattern can act both as bioadhesive region for selective cell adhesion and as nanocarrier for drug molecules to regulate cell behaviors. Quantitative analysis of cell adhesion shows that selective HepG2 cell adhesion and spreading are promoted by the micropatterned MgAl-LDH, and also suppressed by methotrexate drug released from the LDH interlayer galleries.

KEYWORDS: layered double hydroxide, micropatterned arrays, photolithography, in situ growth, cell adhesion, methotrexate



Surface micropatterning has generated diverse scientific and technological interests in various application fields in cell biology.^{1–3} Cell adhesion defined on micropatterned surfaces has been utilized in biosensors, tissue engineering, and drug screening, as well as understanding of fundamental questions concerning cell biology. To selectively localize cells adhesion, various micropatterned bioadhesive surfaces have been successfully created on the basis of soft and photolithography-based surface micropatterning techniques.^{4–11} For example, selective cell adhesion was regulated by hydrophobic self-assembled monolayers (SAMs) of alkanethiols on gold substrate;⁷ however, with the limited stability under cell culture conditions. Functionalized poly(ethylene glycol) (PEG) backbone polymers,⁸ combined with photolithography, were found to significantly improve selective cell attachment, however, the necessity of multiple plasma processes and expensive apparatuses, or the drawbacks of the mediocre stability under cell-culture condition, results from the physisorbed PEG coating. Inorganic biomimetic micropatterns, such as hydroxyapatite (HAp)⁹ and calcium carbonate (CaCO_3),^{3,10} have also been investigated as promising cell-adhesive micropatterns to dramatically enhance cell adhesion and spreading, however, the physisorbed molecular template to the formation of inorganic micropatterns may not match long-term mechanical properties and interaction with the surrounding tissue.¹¹ These problems could be mitigated if facile synthetic approaches are needed in developing biomimetic micropatterns that strongly bonded to the underlying substrate surface.

Layered double hydroxides (LDHs), well-known as a class of hydroxide-like anionic inorganic compounds,¹² have been

shown to be promising biocompatible materials in applications such as biosensor and drug/gene delivery. LDHs are represented typically by formula $[\text{M}^{\text{II}}_{1-x}\text{M}^{\text{III}}_x(\text{OH})_2](\text{A}^{n-})_{x/n} \cdot m\text{H}_2\text{O}$, where M^{II} and M^{III} are divalent and trivalent metal cations, respectively, and A^{n-} is an exchangeable anion between the hydrated interlayer galleries. Distinctly different from other inorganic biocompatible materials such as HAp and CaCO_3 , a major advantage of LDHs is the versatility in varying the metal cations, the $\text{M}^{\text{II}}/\text{M}^{\text{III}}$ molar ratio, cation distribution, and especially the exchangeable interlayer anions over a wide range. Various theoretical¹³ and experimental^{14–25} studies have demonstrated that anion-exchangeable LDHs are able to act as potential biocompatible inorganic host, either via direct nanocarrier for various drugs (such as methotrexate (MTX)¹⁴ and ibuprofen¹⁵) and gene molecules (such as DNA^{16,17} and siRNA^{18,19}), or via surface-modification of LDHs for drug delivery by using ligand,²⁰ siRNA,²¹ and inorganic gold nanoparticle.²² However, all drug- or gene/LDH hybrids for drug/gene delivery were involved in the form of LDH nanoparticles. Recently, a pristine MgFe-LDH continuous film grown directly on Mg substrate was found to facilitate cell spreading.²³ Despite their potential, cells cultured on the MgFe-LDH continuous film, which are free to adopt any spreading, are in marked contrast to those on micropatterning confinement in which cells can further be forced to span across nonadhesive regions to adhesive regions, a frequently

Received: January 9, 2015

Accepted: February 5, 2015

Published: February 5, 2015



Scheme 1. Schematic Illustration of MgAl-LDH Micropatterned Arrays for Regulating Cell Adhesion, Involving Surface Modification, Selective UV Irradiation via a Photomask, and in situ Growth of LDH Micropatterns under Hydrothermal Conditions, as well as Cell Incubation in DMEM without and with Release of MTX Drug Molecules

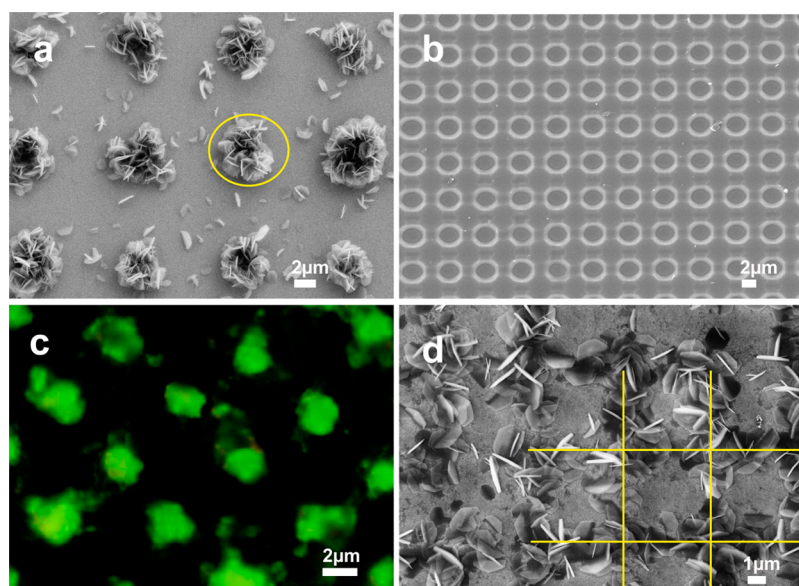
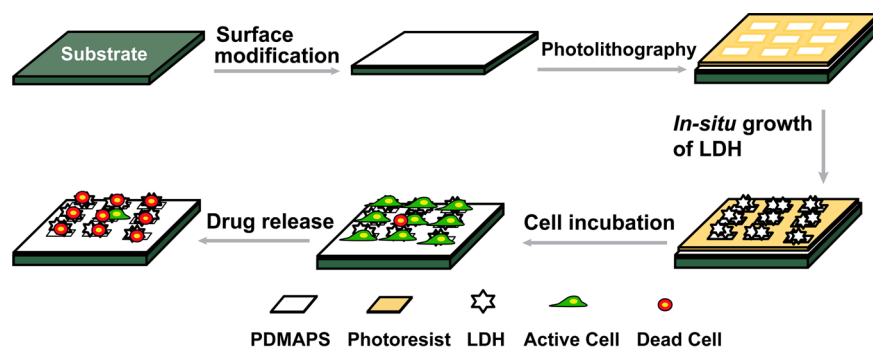


Figure 1. SEM images of (a) MgAl-LDH micropatterned arrays grown on gold substrate, (b) the negative patterns upon exposure of the photoresist on gold substrate, (c) fluorescent micrograph of BSA protein adsorbed selectively on LDH micropatterned arrays from a, and (d) gridlike LDH micropatterns obtained fancily by altering photomask. The yellow markers are superimposed on the SEM images of LDH micropatterned arrays.

encountered in vivo scenario. Especially, in the context of potential application for biosensor and microfluidic devices, cell micropatterning could be used to realize highly intensive detection in a limited field with a great density detection unit. Additionally, the Mg-based substrate was not ready to allow for direct cell imaging and monitoring.^{5,24}

We have recently shown that zwitterionic poly(3-dimethyl (methacryloyloxyethyl) ammoniumpropanesulfonate) (PDMAAPS)-functionalized LDH nanoparticles exhibited a highly enhanced hemocompatibility.²⁵ In this Letter, we describe a reliable preparation of MgAl-LDH micropatterned arrays strongly bonded to supporting gold substrate by combining SO_3^- -terminated self-assembly monolayer (SAM) and photolithography. The SO_3^- -based synthesis route is also readily extended to the in situ growth of MgAl-LDH micropatterned arrays on the above SO_3^- -terminated PDMAAPS-immobilized glass substrate, which could be amenable for cell imaging (Scheme 1). Distinctly, the anion-exchangeable micropatterned MgAl-LDH is expected to play a dual role in acting both as a bioadhesive region for selective cell adhesion and as a nanocarrier for drug molecules to control cell behavior. Optical observation and quantitative analysis of

HepG2 cell adhesion are examined in terms of micropatterned MgAl-LDH arrays without and with the release of MTX drug from the LDH interlayer galleries.

MgAl-LDH micropatterned arrays were prepared under hydrothermal conditions via combining surface modification and photolithography (See the experimental details in the Supporting Information). In brief, the micropatterned MgAl-LDH arrays were prepared by surface modification of the gold substrate with $\text{HS}(\text{CH}_2)_3\text{SO}_3^-$ -terminated SAM, subsequent photolithography, exposure of the negative micropatterned photoresist, and in situ growth of LDHs under hydrothermal conditions, as well as removal of the unexposed micropatterned photoresist. The formation of the MgAl-LDH grown on the underlying gold substrate is confirmed by the XRD patterns of the LDHs precipitate collected from the aqueous solution (see Figure S1 in the Supporting Information). The strong basal reflections of (001) were observed at low angle values, and nonbasal (110) and (113) reflections at high angle values, clearly confirming the highly crystalline and typical layered feature of the LDH formed on the gold substrate. Scanning electron microscopy (SEM) image shows that each rose-like LDH array is confined within one exposed negative pattern

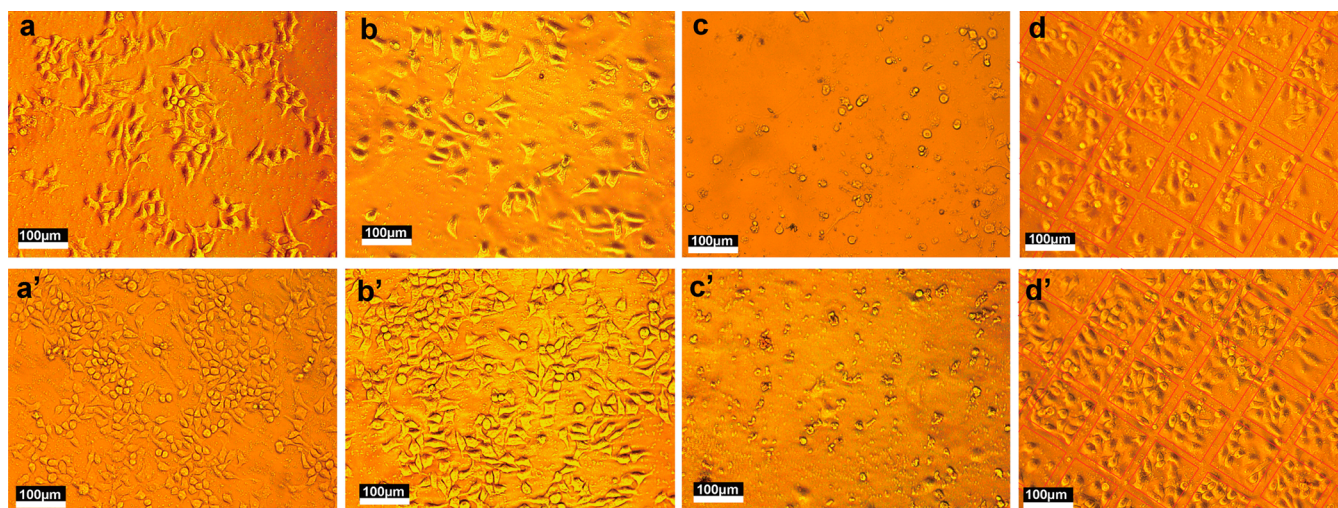


Figure 2. Optical micrographs of HepG2 cells on different glass substrates: (a, a') pure glass, (b, b') LDH film-modified, (c, c') PDMAPS-modified, and (d, d') pure MgAl-LDH micropatterned arrays without intercalated MTX. The different periods of incubation range from 12 h (panels a, b, c, and d) to 24 h (panels a', b', c', and d'). The red markers in d and d' are superimposed to the profiles of the MgAl-LDH micropatterned arrays to confine the cells.

(Figure 1a). The mean center-to-center distance between two roselike LDH arrays was measured to be $5.4 \mu\text{m}$, quantitatively fitting that ($5.5 \mu\text{m}$) of the circlelike negative micropatterns after exposure of the photoresist (Figure 1b). Few MgAl-LDH platelets were also observed to scatter between the roselike LDH arrays, possibly because of the loosely adsorbed aggregates. No formation of the roselike LDH on the unexposed PMMA photoresist region can be ascribed to that PMMA, with $-\text{CH}_3$ terminal group, could neither adsorb the cations of Mg^{2+} and Al^{3+} , nor further facilitate the nucleation or growth of MgAl-LDH nanoplatelets under hydrothermal conditions. The resistance of $-\text{CH}_3$ terminal group is confirmed experimentally by the fact that no LDH platelet was observed to grow on the $\text{HS}(\text{CH}_2)_3\text{CH}_3$ SAM-modified gold surface (Figure S2 in the Supporting Information). The selective growth of the LDH arrays can thus be attributed to the templating role of the $-\text{SO}_3^-$ -terminated SAM within the negative micropatterned circles upon exposure. The morphology of the LDH micropattern is supported by confocal laser scanning microscopy image of fluorescein isothiocyanate-labeled bovine serum albumin (BSA) protein upon physical adsorption. A uniform distribution of green-labeled BSA was clearly observed (Figure 1c) selectively onto the MgAl-LDH patterned arrays with hydroxyl-rich terminal groups.

This $-\text{SO}_3^-$ -SAM-based synthesis route was readily extended to prepare different LDH micropatterned arrays. By varying the predesigned photomask pattern, a gridlike LDH micropattern was easily obtained (Figure 1d) with a dimensional size of $3.3 \mu\text{m}$. The gridlike micropatterns show a flexibility in designing various LDH-based arrays toward desired morphological micropatterns, which are readily achieved by using photomasks with tunable dimensional sizes and geometries.

Furthermore, the versatile synthesis route was employed to prepare MgAl-LDH micropatterned arrays on glass substrate, which is amenable to be *in vitro* observed and also to improve cell imaging.²⁴ In this case, surface modification of the precleaned glass substrate was altered by using PDMAPS with $-\text{SO}_3^-$ end groups reported in our early study.²⁵ XRD patterns (Figure S3a in the Supporting Information) show the characteristic (003) and (006) reflections of the resultant LDH

grown on the glass substrate (JCPDS File No. 38-0487), consistent with a previous study of the LDH films grown on the poly(vinyl alcohol)-modified glass substrate.²⁶ Also, this LDH formation is evidenced by the hydroxalite-like XRD patterns of the LDHs powder scraped from the glass substrate, as shown in Figure S3b in the Supporting Information. SEM observations show that squarelike micropatterned LDH arrays were grown on the PDMAPS-functionalized region, with a mean dimensional size of $100 \mu\text{m}$ and a space interval of $20 \mu\text{m}$ (Figure S4 in the Supporting Information). This selective growth confirms again the role of $-\text{SO}_3^-$ end groups in guiding the selective growth of LDH on the glass substrate. Note that small defects of LDH micropatterns were observed, possibly because of the decreased surface density of the DMAPS grafted on the glass substrate when compared with the SAM on the gold substrate.

Adhesion of HepG2 cells was examined to evaluate the biocompatibility of the LDH micropatterned arrays without MTX intercalated between the LDH interlayer galleries. HepG2 cell was chosen for this study because of the general utilization in pharmaceutical studies.²⁷ Basically, this spindlelike shape of the cell spreading indicates the viability originated from a proper adhesion between cell and the surface.²⁸ Different substrates were dipped into Dulbecco's modified eagle medium (DMEM) with HepG2 cells for different periods of incubation, and the cell shape was observed by using optical microscopy, as reported previously.⁷ We first evaluated adhesion of HepG2 cells on the pure glass, PDMAPS-modified and LDH film-modified glass substrates. Upon 12 h of incubation, the cells are distributed randomly, with a spindle-like shape on the LDH film-coated, and pristine glass substrates (Figure 2a and 2b), but with a spherical shape on the PDMAPS-functionalized glass substrate (Figure 2c). On the basis of this significant difference in cell shape, we believe that the PDMAPS-functionalized surface is resistant to cell adhesion, whereas LDH continuous film is amenable to HepG2 cell adhesion. The role of MgAl-LDH film is indeed consistent with previous study of the MgFe-LDH continuous film capable of facilitating cell spreading.²³ When the incubation time was increased to 24 h, the cells were found to increase on the pure and LDH film-modified glass substrates,

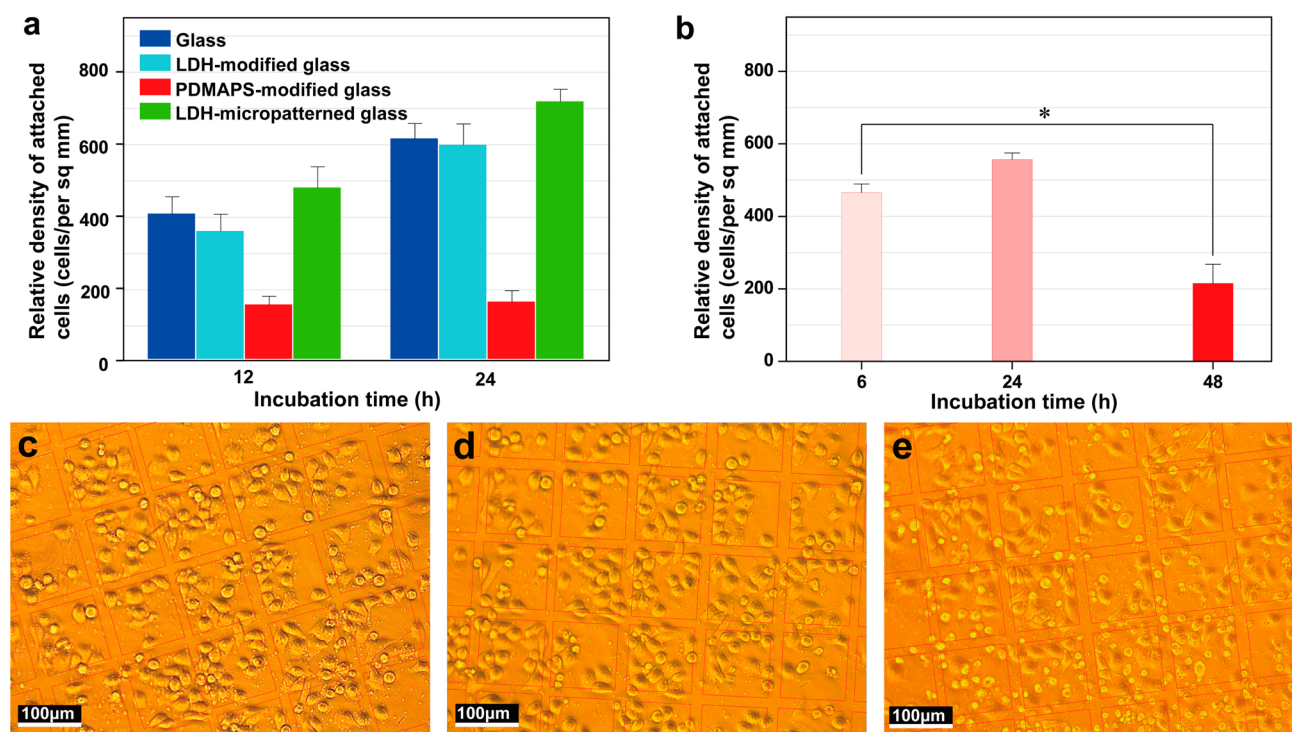


Figure 3. Relative density of cell adhesion (cells/per sq mm) of (a) different substrate: pure glass, LDH film-modified, and PDMAPS-modified glass substrates, and pure LDH micropatterned array glass substrate, after incubation of 12 and 24 h, and (b) the MTX/LDH micropatterned arrays with intercalated MTX, after incubation of 6, 24, and 48 h (mean \pm SD, $n = 3$, $*p < 0.05$). And optical micrographs of HepG2 cell adhesion on MTX/LDH micropatterned arrays with intercalated MTX, after incubation for (c) 6, (d) 24, and (e) 48 h. The red markers are superimposed to the profiles of the LDH micropatterns to confine the cells.

both with a spindle-like shape (Figure 2a', b'). However, the cells on the PDMAPS-functionalized glass substrate still preserve a spherical shape (Figure 2c'), similar to the above result upon 12 h of incubation (Figure 2c).

Quantitative analysis of cell adhesion was performed by determining the relative cell-adhesion density (cell/per sq mm) on the different glass substrates using a hemocytometer. In the case of the pure glass and LDH film-modified glass substrates, the values of the relative cell adhesion density are increased remarkably from 407 to 615 cells/per sq mm, and from 359 to 598 cells/per sq mm, respectively (Figure 3a). However, no change in number of the cells on the DMAPS-modified glass substrate was found, i.e., from 155 to 163 cells/per sq mm through an incubation interval of 12 h (Figure 3a). We therefore suggest that the LDH film-modified glass substrate is able to act as a bioadhesive region and nonselectively promote the adhesion and growth of HepG2 cells.

To mimic confined environment to cell adhesion and thereby to selectively localize cells adhesion, we further designed and prepared MgAl-LDH micropatterned arrays as a bioadhesive region on the PDMAPS-functionalized glass substrate. On the basis of the different roles in cell adhesion between the LDH film- and PDMAPS-functionalized glass substrates, the $-\text{SO}_3^-$ -terminated PDMAPS polymer brushes is designed to play a dual role in acting both as template to guide selective growth of LDH micropatterned arrays chemically bonded to the glass substrate, and as a nonadhesive region for effective resistance to cell adhesion. We then examined HepG2 cell adhesion on the pristine LDH array-micropatterned glass substrate without intercalated MTX. HepG2 cells were found to regularly disperse onto the LDH micropatterned arrays after the first 12 h of incubation, as shown by the superimposed markers in

Figure 2d. Especially, after 24 h of incubation, HepG2 cells are still confined regularly within the LDH micropatterns (Figure 2d'), considering that effect of small defects of LDH micropatterns on cell adhesion could be neglected when compared with the large dimensional size of cells. Quantitatively, the spreading cell adhesion density is increased from 479 to 718 cells/per sq mm after the incubation periods from 12 to 24 h (Figure 3a). We therefore conclude that the MgAl-LDH micropatterned array is capable of selectively confining cell spreading, and also favoring the cell adhesion and growth. The possibilities of the improvement could be assigned to the biocompatibility of the hydroxyl-rich LDH layer, and also mainly to the roughness of the micropatterned arrays. This benefit is indeed consistent with a similar improvement on cell spreading onto the rough MgAl-LDH film²³ and Hap micropattern arrays⁹ reported previously. We also checked the cell shapes and LDH micropatterns after 48 h of incubation. No significant changes in cell shape and number were found, or no LDH dissolution/recrystallization was observed on the glass substrate in DMEM environment. Also, no delamination or peeling of LDH nanoplatelets was observed to occur upon cross-cutting the LDH micropattern surface. The results reveal the chemical and mechanical stability of LDH micropatterned arrays used for cell culture.

From numerous previous studies,^{14–19} it is well-known that the unique anion-exchangeable LDHs nanoparticles are capable of acting as nanocarriers for drug molecules and controlled delivery of drug molecules. We then evaluated cell suppression of the MTX-intercalated MgAl-LDH (MTX/LDH) micropatterned arrays cultured in DMEM. MTX was chosen as a model drug due to high suppression effect of the proliferation of cells and relatively low toxicity.^{12,14,29} MTX-intercalated

LDH (MTX/LDH) micropatterned arrays were first prepared (See the Experimental section in the Supporting Information). On the basis of the XRD patterns of the powder scraped from MTX/LDH micropatterned arrays on the glass substrate, the basal peaks of (001) were observed to shift to lower angles (less than 10°) after MTX intercalation (Figure S5a in the Supporting Information), when compared with those centered typically at $2\theta > 11.6^\circ$ which correspond to the intercalation of CO_3^{2-} anions of the pristine MgAl-LDH micropatterned arrays (shown in Figure S3 in the Supporting Information). This remarkable shift clearly reveals the intercalation²⁹ of MTX between the LDH interlayer galleries of the MgAl-LDH micropatterned array. After different periods of incubation in DMEM, the cells were also found to be confined onto the MTX/LDH micropatterned arrays, with both spindle- and roundlike shapes for 6 and 24 h (Figures 3c, d), however, with increasing roundlike shapes for 48 h (Figure 3e).

Quantitatively, Figure 3b shows that the relative cell-adhesion density of the spindle-like spreading cells are first increased and then decreased with increasing incubation periods, i.e., ranging from 526 cells/per sq mm for the initial 6 h, 557 cells/per sq mm for 24 h; however, the density is eventually down to 215 cells/per sq mm for 48 h. The decrease can be due to the increasing release of MTX molecules from the LDH interlayer galleries.^{14,29} To support this hypothesis, we examined the release of MTX from the MTX/LDH micropatterned arrays. Release behavior of MTX was found to be very rapid within first 6 h in DMEM, followed by a very slow release of MTX up to a subsequent period of 14 h (Figure S6 in the Supporting Information), in good agreement with a previous study of a two-step release behavior of MTX.³⁰ The release of MTX can be evidenced by the XRD result of the powder scraped from MTX/LDH micropatterned arrays after 48 h of incubation in DMEM. In this case, the basal reflection peaks of (001) was observed to shift to higher angles centered at $2\theta > 11.6^\circ$ (Figure S5b in the Supporting Information), when compared with those ($2\theta < 10^\circ$) of the MTX-intercalated LDH micropatterned arrays (as shown in Figure S5a in the Supporting Information). The remarkable shift strongly reveals the anion exchange of MTX with CO_3^{2-} anions in DMEM. Upon approaching completion of MTX release to DMEM, the concentration of MTX reaches increasing levels in DMEM, and the growth of cells is inhibited significantly.

In summary, we have explored a reliable synthesis route of LDH micropatterned arrays on gold substrate by combining surface modification and photolithography, and further extended the micropatterned preparation on glass substrates to mimic the confined environment of cell adhesion. By virtue of the unique dual roles in biocompatibility and nanocarrier of anion-exchangeable MgAl-LDH, HepG2 cell adhesion is able to be steered in a controlled manner: promoted by the pristine LDH micropatterned arrays, and further suppressed by MTX drug released from the MTX/LDH micropatterned arrays. This LDH micropatterned arrays enable the regulation of cell adhesion and may be a potentially powerful tool for regulating cells inside microfluidic devices for biological applications.

■ ASSOCIATED CONTENT

Supporting Information

Experimental section, XRD patterns, and SEM images. This material is available free of charge via the Internet at <http://pubs.acs.org>.

■ AUTHOR INFORMATION

Corresponding Authors

*E-mail: xusl@mail.buct.edu.cn.

*E-mail: xufj@mail.buct.edu.cn.

Author Contributions

[†]F.Y. and H.H. contributed equally to this work.

Notes

The authors declare no competing financial interest.

■ ACKNOWLEDGMENTS

We greatly thank Prof. Feng Shi for assistance in photolithography technique. This work was financially supported by National Basic Research Program of China (973 Program, 2014CB932102), the National Natural Science Foundation of China (21071012 and 51325304), and Beijing Engineering Center for Hierarchical Catalysts, as well as Collaborative Innovation Center for Cardiovascular Disorders, Beijing Anzhen Hospital Affiliated to the Capital Medical University.

■ REFERENCES

- (1) Yao, X.; Peng, R.; Ding, J. Cell-Material Interactions Revealed via Material Techniques of Surface Patterning. *Adv. Mater.* **2013**, *25*, 5257–5286.
- (2) Lee, K.; Wagermaier, W.; Masic, A.; Kommareddy, K. P.; Bennet, M.; Manjubala, I.; Lee, S.-W.; Park, S. B.; Cölfen, H.; Fratzl, P. Self-Assembly of Amorphous Calcium Carbonate Microlens Arrays. *Nat. Commun.* **2012**, *3*, 725–731.
- (3) Lee, H. J.; Kim, D. N.; Park, S.; Lee, Y.; Koh, W.-G. Micropatterning of a Nanoporous Alumina Membrane with Poly(ethylene glycol) Hydrogel to Create Cellular Micropatterns on Nanotopographic Substrates. *Acta Biomater.* **2011**, *7*, 1281–1289.
- (4) Guo, Z.; Hu, K.; Sun, J.; Zhang, T.; Zhang, Q.; Song, L.; Zhang, X.; Gu, N. Fabrication of Hydrogel with Cell Adhesive Micropatterns for Mimicking the Oriented Tumor-Associated Extracellular Matrix. *ACS Appl. Mater. Interfaces* **2014**, *6*, 10963–10968.
- (5) You, J.; Shin, D.-S.; Patel, D.; Gao, Y.; Revzin, A. Multilayered Heparin Hydrogel Microwells for Cultivation of Primary Hepatocytes. *Adv. Healthcare Mater.* **2014**, *3*, 126–132.
- (6) Sterner, O.; Giazoni, M.; Zurcher, S.; Tosatti, S.; Liley, M.; Spencer, N. D. Delineating Fibronectin Bioadhesive Micropatterns by Photochemical Immobilization of Polystyrene and Poly(vinylpyrrolidone). *ACS Appl. Mater. Interfaces* **2014**, *6*, 18683–18692.
- (7) Kim, D. J.; Lee, J. M.; Park, J.-G.; Chung, B. G. A Self-Assembled Monolayer-Based Micropatterned Array for Controlling Cell Adhesion and Protein Adsorption. *Biotechnol. Bioeng.* **2011**, *108*, 1194–1202.
- (8) Mohr, J. C.; de Pablo, J. J.; Palecek, S. P. 3-D Microwell Culture of Human Embryonic Stem Cells. *Biomaterials* **2006**, *27*, 6032–6042.
- (9) He, Y.; Wang, X.; Chen, L.; Ding, J. Preparation of Hydroxyapatite Micropatterns for the Study of Cell-Biomaterial Interactions. *J. Mater. Chem. B* **2014**, *2*, 2220–2227.
- (10) Kumar, P. T. S.; Ramya, C.; Jayakumar, R.; Nair, S. k. V.; Lakshmanan, V.-K. Drug Delivery and Tissue Engineering Applications of Biocompatible Pectin-Chitin/Nano CaCO_3 Composite Scaffolds. *Colloid Surf., B* **2013**, *106*, 109–116.
- (11) Wu, X.; Wang, S. Biomimetic Calcium Carbonate Concentric Microgrooves with Tunable Widths for Promoting MC3T3-E1 Cell Functions. *Adv. Healthcare Mater.* **2013**, *2*, 326–333.
- (12) Choi, S.-J.; Oh, J.-M.; Choy, J.-H. Human-Related Application and Nanotoxicology of Inorganic Particles: Complementary Aspects. *J. Mater. Chem.* **2008**, *18*, 615–620.
- (13) Thyveetil, M.-A.; Coveney, P. V.; Greenwell, H. C.; Suter, J. L. Computer Simulation Study of the Structural Stability and Materials Properties of DNA-Intercalated Layered Double Hydroxides. *J. Am. Chem. Soc.* **2008**, *130*, 4742–4756.

(14) Choi, G.; Kwon, O.-J.; Oh, Y.; Yun, C.-O.; Choy, J.-H. Inorganic Nanovehicle Targets Tumor in an Orthotopic Breast Cancer Model. *Sci. Rep.* **2014**, *4*, 4430–4336.

(15) Khan, A. I.; Lei, L.; Norquist, A. J.; O'Hare, D. Intercalation and Controlled Release of Pharmaceutically Active Compounds from a Layered Double Hydroxide. *Chem. Commun.* **2001**, *37*, 2342–2343.

(16) Choy, J.-H.; Kwak, S.-Y.; Park, J.-S.; Jeong, Y.-J.; Portier, J. Intercalative Nanohybrids of Nucleoside Monophosphates and DNA in Layered Metal Hydroxide. *J. Am. Chem. Soc.* **1999**, *121*, 1399–1400.

(17) Desigaux, L.; Ben Belkacem, M.; Richard, P.; Cellier, J.; Leone, P.; Cario, L.; Leroux, F.; Taviot-Gueho, C.; Pitard, B. Self-Assembly and Characterization of Layered Double Hydroxide/DNA Hybrids. *Nano Lett.* **2006**, *6*, 199–204.

(18) Ladewig, K.; Niebert, M.; Xu, Z. P.; Gray, P. P.; Lu, G. Q. M. Efficient siRNA Delivery to Mammalian Cells Using Layered Double Hydroxide Nanoparticles. *Biomaterials* **2010**, *31*, 1821–1829.

(19) Wong, Y.; Markham, K.; Xu, Z. P.; Chen, M.; Lu, G. Q.; Bartlett, P. F.; Cooper, H. M. Efficient Delivery of siRNA to Cortical Neurons Using Layered Double Hydroxide Nanoparticles. *Biomaterials* **2010**, *31*, 8770–8779.

(20) Oh, J.-M.; Choi, S.-J.; Lee, G.-E.; Han, S.-H.; Choy, J.-H. Inorganic Drug-Delivery Nanovehicle Conjugated with Cancer-Cell-Specific Ligand. *Adv. Funct. Mater.* **2009**, *19*, 1617–1624.

(21) Li, L.; Gu, W.; Chen, J.; Chen, W.; Xu, Z. P. Co-delivery of siRNAs and Anti-Cancer Drugs Using Layered Double Hydroxide Nanoparticles. *Biomaterials* **2014**, *35*, 3331–3339.

(22) Wang, L.; Xing, H.; Zhang, S.; Ren, Q.; Pan, L.; Zhang, K.; Bu, W.; Zheng, X.; Zhou, L.; Peng, W.; Hua, Y.; Shi, J. A Gd-Doped Mg-Al-LDH/Au Nanocomposite for CT/MR Bimodal Imagings and Simultaneous Drug Delivery. *Biomaterials* **2013**, *34*, 3390–3401.

(23) Lin, J.-K.; Uan, J.-Y.; Wu, C.-P.; Huang, H.-H. Direct Growth of Oriented Mg-Fe Layered Double Hydroxide (LDH) on Pure Mg Substrates and in Vitro Corrosion and Cell Adhesion Testing of LDH-Coated Mg Samples. *J. Mater. Chem.* **2011**, *21*, 5011–5020.

(24) Shah, S. S.; Howland, M. C.; Chen, L.-J.; Silangcruz, J.; Verkhoturov, S. V.; Schweikert, E. A.; Parikh, A. N.; Revzin, A. Micropatterning of Proteins and Mammalian Cells on Indium Tin Oxide. *ACS Appl. Mater. Interfaces* **2009**, *1*, 2592–2601.

(25) Hu, H.; Wang, X. B.; Xu, S. L.; Yang, W. T.; Xu, F. J.; Shen, J.; Mao, C. Preparation and Evaluation of Well-defined Hemocompatible Layered Double Hydroxide-Poly(sulfobetaine) Nanohybrids. *J. Mater. Chem.* **2012**, *22*, 15362–15369.

(26) Guo, X.; Zhang, F.; Xu, S.; Evans, D. G.; Duan, X. Preparation of Layered Double Hydroxide Films with Different Orientations on the Opposite Sides of a Glass Substrate by in situ Hydrothermal Crystallization. *Chem. Commun.* **2009**, *45*, 6836–6838.

(27) Zeng, Q.; Zhang, Y.; Ji, W.; Ye, W.; Jiang, Y.; Song, J. Inhibition of Cellular Toxicity of Gold Nanoparticles by Surface Encapsulation of Silica Shell for Hepatocarcinoma Cell Application. *ACS Appl. Mater. Interfaces* **2014**, *6*, 19327–19335.

(28) Stach, M.; Kronekova, Z.; Kasak, P.; Kollar, J.; Pentrak, M.; Micusik, M.; Chorvat, D., Jr.; Nunney, T. S.; Lacik, I. Polysulfobetaine Films Prepared by Electrografting Technique for Reduction of Biofouling on Electroconductive Surfaces. *Appl. Surf. Sci.* **2011**, *257*, 10795–10801.

(29) Oh, J.-M.; Choi, S.-J.; Kim, S.-T.; Choy, J.-H. Cellular Uptake Mechanism of An Inorganic Nanovehicle and Its Drug Conjugates: Enhanced Efficacy Due to Clathrin-Mediated Endocytosis. *Bioconjugate Chem.* **2006**, *17*, 1411–1417.

(30) Qi, F.; Zhang, X.; Li, S. A Novel Method to Get Methotrexatum/Layered Double Hydroxides Intercalation Compounds and Their Release Properties. *J. Phys. Chem. Solids* **2013**, *74*, 1101–1108.